Albumin Biomolecular Drug Designs Stabilized through Improved Thiol Conjugation and a Modular Locked Nucleic Acid Functionalised Assembly

Anders Dinesen [a], Alexander Winther [a], Archie Wall [b], Anders Märcher [a], Johan Palmfeldt [c], Vijay Chudasama [b], Jesper Wengel [d], Kurt V. Gothelf [a,e], James R. Baker [b], and Kenneth A. Howard [a,f,*]

[a] Interdisciplinary Nanoscience Center (iNANO), Aarhus University, DK-8000 Aarhus C, Denmark
[b] Department of Chemistry, University College London, London, WC1H 0AJ, UK
[c] Research Unit for Molecular Medicine, Department of Clinical Medicine, Aarhus University and Aarhus University Hospital, DK-8200 Aarhus N, Denmark
[d] Nucleic Acid Center, Department of Physics, Chemistry, and Pharmacy, University of Southern Denmark, DK-5230 Odense M, Denmark
[e] Department of Chemistry, Aarhus University, DK-8000 Aarhus C, Denmark
[f] Department of Molecular Biology and Genetics, Aarhus University, DK-8000 Aarhus C, Denmark
* Correspondence: kenh@inano.au.dk

Abstract

Albumin-nucleic acid biomolecular drug designs offer modular multifunctionalisation and extended circulatory half-life. However, stability issues associated with conventional DNA nucleotides and maleimide bioconjugation chemistries limit the clinical potential. This work aims to improve the stability of this thiol conjugation and nucleic acid assembly by employing a fast-hydrolysing monobromomaleimide (MBM) linker and nuclease-resistant nucleotide analogues, respectively. The biomolecular constructs were formed by site-selective conjugation of a 12-mer oligonucleotide to cysteine 34 (Cys34) of recombinant human albumin (rHA), followed by annealing of functionalised complementary strands bearing either a fluorophore or the cytotoxic drug monomethyl auristatin E (MMAE). Formation of conjugates and assemblies were confirmed by gel shift analysis and mass spectrometry, followed by investigation of serum stability, neonatal Fc receptor (FcRn)-mediated cellular recycling, and cancer cell killing. The MBM linker afforded rapid conjugation to rHA and remained stable during hydrolysis. The albumin-nucleic acid biomolecular assembly composed of stabilised oligonucleotides exhibited high serum stability and retained FcRn engagement mediating FcRn-mediated cellular recycling. The MMAE-containing assembly exhibited cytotoxicity in the human MIA PaCa-2 pancreatic cell line with an IC50 of 342 nM, triggered by drug release from breakdown of an acid-labile linker. In summary, this work presents rHA-nucleic acid module-based assemblies with improved stability and retained module functionality that further promotes the drug delivery potential of this biomolecular platform.

Keywords: Biomolecular drug designs; albumin; nucleic acids; bioconjugation; stability; half-life extension.

1. Introduction

Low molecular weight drugs and biomacromolecules are susceptible to rapid renal clearance, and can, therefore, require half-life extension technologies to prolong their therapeutic effect [1, 2]. Approaches to achieve this include the use of poly(ethylene glycol) (PEG) [3] or protein conjugation [4]. An attractive half-life extension approach utilises albumin due to its extended circulatory half-life of approximately 19 days facilitated by engagement with the cellular recycling neonatal Fc receptor (FcRn) [5]. Several albumin-binding drugs, albumin fusions, and albumin conjugates are on the market or are in clinical trials [2, 6, 7]. Site-selective conjugation of maleimide-functionalised drugs to albumin's single free thiol at cysteine 34 (Cys34) in

albumin's domain I, distant from the main FcRn interaction interface at domain III, minimises interference with the FcRn-mediated recycling process [8]. The reaction of maleimides' strong electrophilic carbon-carbon double bond with the nucleophilic thiolate on cysteine, forming a thiosuccinimide, is the fastest Michael addition reaction [9-12] and is widely used to conjugate drugs to proteins [13, 14] including albumin [15] through bifunctional linkers or maleimide-functionalised drugs. The thiosuccinimide formed by the maleimide-thiol reaction, however, is susceptible to cleavage through a retro-Michael reaction reforming the starting maleimide that can undergo inactivating hydrolysis or thiol exchange in presence of excess thiols [16, 17]. This has been shown in *in vivo* studies by both Shen *et al*. [18] and Jackson *et al*. [19] where antibody-drug conjugates (ADCs) prematurely released or re-conjugated their payloads to endogenous thiols on albumin. This can be prevented by hydrolyzing the thiosuccinimide leading to a ring opening forming a stable succinamic acid thioether [20, 21]. However, as shown by the Baker and Chudasama groups, hydrolysis can lead to loss of around half of the conjugate due to retro-Michael [22]. Therefore, several next-generation maleimides have been developed [23] including the monobromomaleimide (MBM) first developed by Baker and colleagues in 2009 [24]. The bromine acts as a leaving group during conjugation to a thiol, preserving the maleimide unsaturation to form a thiomaleimide that prevents the retro-Michael reaction (Figure S1) [22]. Further, the design of the MBM-linker has been optimised to increase the rate of hydrolysis, facilitating production of stable thioether adducts in the conjugates [25].

Single-site attachment at albumin's Cys34 limits drug payload capacity and inclusion of additional functional groups such as targeting moieties. Conjugation of nucleic acids to Cys34 allows generation of assemblies that act as scaffolds for incorporation of multiple drugs or functional groups into an albumin-nucleic acid biomolecular drug design [26]. Complementary strands bearing different functional groups offer a selective module-based approach for a specific application. We have previously introduced an albumin-nucleic acid biomolecular platform for functionalisation with drugs or imaging agents using site-selective conjugation to Cys34 with standard maleimide chemistry [26]. However, this construct was comprised of DNA oligonucleotides susceptible to nuclease degradation, limiting its translational potential. The inclusion of locked nucleic acid (LNA) [27, 28], 2'-O-methyl (2'-O-Me) [29], and phosphorothioate (PS) [30] nucleotide modifications preventing nuclease degradation offers a solution.

In this work, we address the stability issues of albumin-DNA biomolecular assemblies by utilising an MBM linker (Figure 1(a)) for irreversible conjugation of nuclease-resistant LNA-, 2'-O-Me, and PS-modified oligonucleotides. A novel MBM-bicyclo[6.1.0]nonyne (BCN) bifunctional linker was employed, as this allows for an efficient and versatile biomolecule conjugation with a tetrazine functionalized oligonucleotide. Biomolecular assemblies containing a fluorophore and the cytotoxic drug monomethyl auristatin E (MMAE) with an acid cleavable linker (Figure 1(b)) were successfully produced and exhibited stability, modular functionality, and FcRn-driven cellular recycling, furthering the translational potential of this biomolecular drug delivery platform.

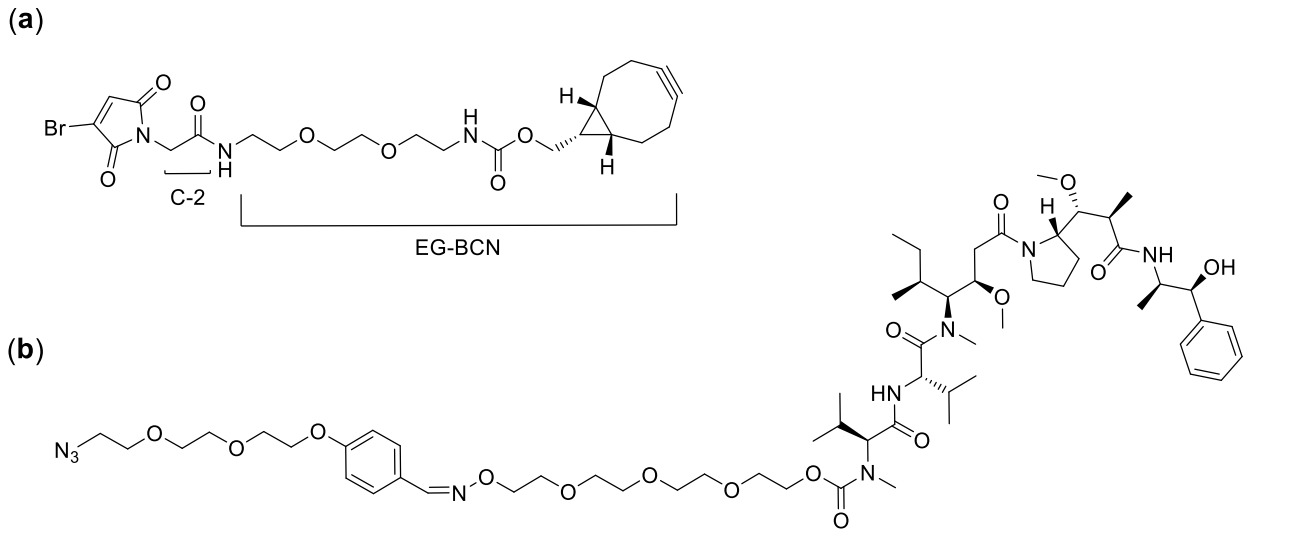

Figure 1. (**a**) Chemical structure of monobromomaleimide (MBM)-bicyclo[6.1.0]nonyne (BCN) linker. C-2: Two-carbon spacer. EG-BCN: Ethylene glycol-BCN. (**b**) Chemical structure of MMAE-azide.

2. Results

2.1. Characterisation of rHA-MBM-linker conjugate

The MBM-BCN linker (Figure 1) was conjugated to rHA, and peptides obtained by trypsinisation were investigated using nanoLC-MS/MS. MS1 scan of the precursor peptide revealed a peptide with a mass corresponding to the Cys34-containing peptide ('ALV peptide', Figure 2) including the mass of the conjugated MBM-BCN-linker (hydrolysed to form the expected maleamic acid, and with the strained alkyne having undergone an oxidation and hydration (+34 Da addition) [31], during the digestion/nano-LC-MS/MS protocol; expected mass: 2944.48, obtained mass: 2944.49 Da). Fragmentation of the ALV peptide confirmed peptide identity and revealed the modification site as being rHA's Cys34 as the mass of only the peptides containing the cysteine (y8-y18, b14, and b20) was increased with a mass corresponding to the MBM-BCN linker (Figure 2)

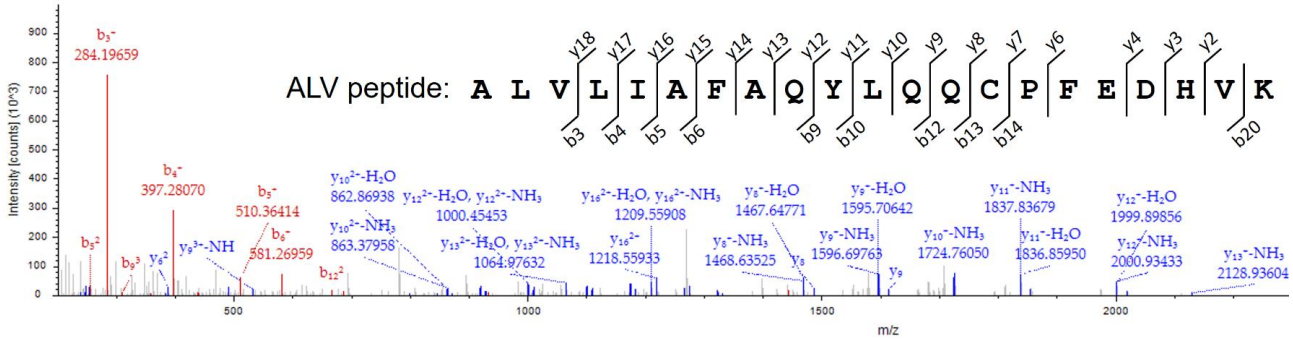

Figure 2. NanoLC-MS/MS data of the rHA-MBM-BCN-linker conjugate. The Cys34-containing 'ALV peptide' of rHA was detected with a mass matching the addition of the MBM-BCN-linker (hydrolysed and with an oxidation of the strained alkyne total monoisotopic peptide mass: 2944.5 Da). After peptide fragmentation the fragments y8-y18, b14, and b20, containing the cysteine, carry the linker modification.

Absorbance at 350 nm was used to monitor thiomaleimide formed by conjugation of the MBM-BCN linker to rHA, yielding a $t_{99\%}$ of ~17 min showing rapid conjugation (Figure 3(a)). Similarly, stabilising hydrolysis of the thiomaleimide to maleamic acid was investigated by the decrease in 350 nm absorbance caused by the

hydrolysis (Figure 3(b)). This indicated fast hydrolysis with a $t_{99\%}$ of ~5 h under relatively mild conditions at pH 8.0 and 37°C. Importantly, it was observed that hydrolysis does not lead to any detectable release of conjugated cargo, suggesting that no retro-Michael reaction occurs (Figure S2).

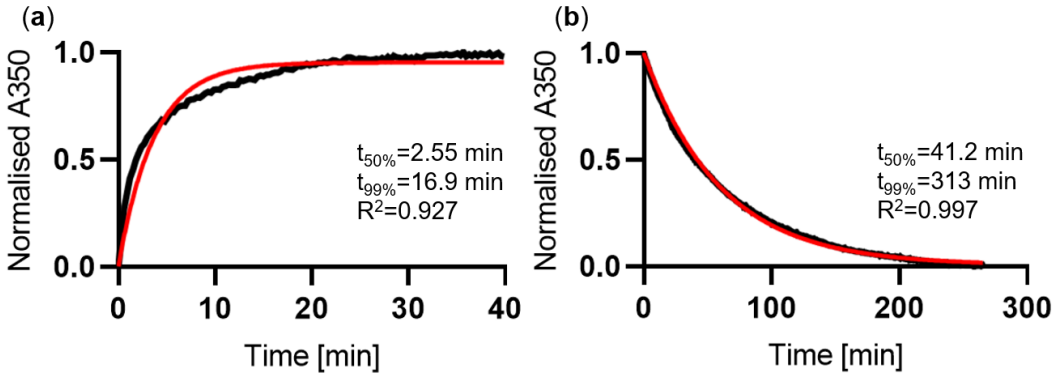

Figure 3. MBM-BCN and rHA reaction and hydrolysis kinetics. Black line: Absorbance data, red line: Data fit. (a) Increasing absorbance at 350 nm indicates formation of thiomaleimide by reaction of MBM-BCN with rHA. (b) Decreasing absorbance at 350 nm indicates hydrolysis of the rHA-conjugated thiomaleimide to maleamic acid.

2.2. Production of albumin-nucleic acid assemblies

The MBM-BCN linker conjugation to rHA was followed by attachment of a Q2 oligonucleotide previously modified with a tetrazine group (Figure S3). The complementary oligonucleotide (cQ2) was functionalised with Cy5.5 or MMAE and then annealed to form the biomolecular assembly.

Modification of the Q2 strand with a tetrazine moiety was shown by mobility shift on a SYBR Gold stained native PAGE (Figure 4(a)). The MBM-BCN linker was conjugated to albumin and, immediately after, conjugated to the tetrazine-modified Q2. HPLC IEX purification was performed to remove excess unconjugated reagents resulting in a pure rHA-Q2 sample (Figure 4(b) lane 3 and (f) peak 3).

cQ2 was functionalised with Cy5.5 or MMAE synthesised in-house with an acid cleavable linker (Figure 1(b)). The linker showed cleavage after incubation at pH 5.5 (Figure S8). Both the Cy5.5 and MMAE conjugates were purified by HPLC RP (Figure 4(g) and (h)) yielding functionalised cQ2 as confirmed by LC-MS (cQ2-Cy5.5 expected mass: 5129.4 Da, obtained mass: 5127.8, cQ2-MMAE expected mass: 6065.6 Da, obtained mass: 6064.1 Da) with high purity confirmed by native PAGE (Figure 4(c) and (d)).

The rHA-Q2 and functionalised cQ2 were annealed with very high efficiency as confirmed by native PAGE yielding two different functionalised albumin-nucleic acid assemblies (Figure 4(e)).

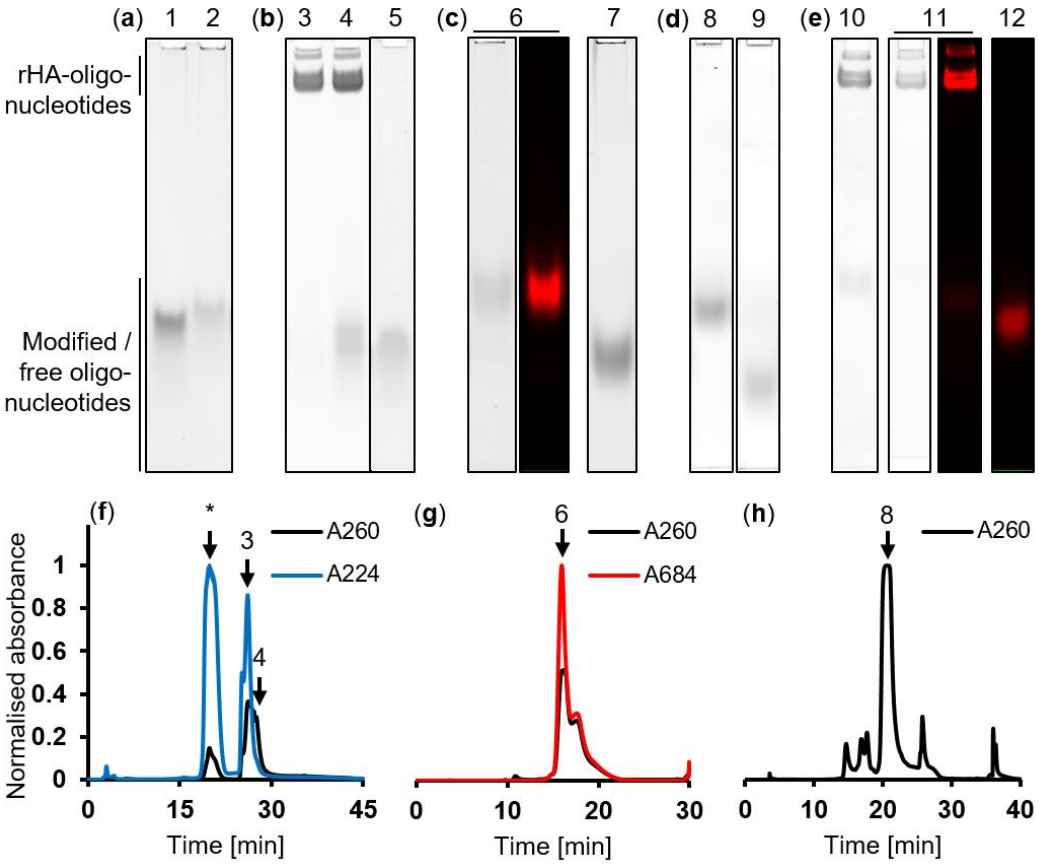

Figure 4. Conjugation and purification of rHA-nucleic acid assemblies. Black bands: SYBR Gold signal, red bands: Cy5.5 fluorescence. A224, A260, and A684 indicate absorbance at 224 nm, 260 nm, and 684 nm, respectively. (**a**): Native PAGE of Q2-tetrazine. Lane 1: Q2, lane 2: Q2-tetrazine. (**b**): Native PAGE of HPLC purification of rHA-MBM-Q2. Lane 3 and 4: HPLC IEX peaks 3 and 4 (as indicated in F), lane 5: Q2-tetrazine control. (**c**): Native PAGE of HPLC purification of cQ2(PS)-Cy5.5. Lane 6: HPLC RP-C18 peak 6 (as indicated in G), Lane 7: cQ2(PS) control. (**d**): Native PAGE of HPLC purification of cQ2(PS)-MMAE. Lane 8: HPLC RP-C18 peak 8 (as indicated in H), lane 9: cQ2(PS) control. (**e**): Native PAGE of annealed albumin-nucleic acid conjugates. Lane 10: WT rHA-MBM-Q2/cQ2(PS)-MMAE, lane 11: WT rHA-MBM-Q2/cQ2(PS)-Cy5.5, lane 12: cQ2(PS)-Cy5.5 control. (**f**): HPLC IEX chromatogram showing purification of rHA-MBM-Q2. * indicates rHA peak. Peaks 3 and 4 were analysed by native PAGE in subfigure (b) lane 3 and 4. (**g**): HPLC RP-C18 chromatogram showing purification of cQ2(PS)-Cy5.5. Peak 6 was analysed by native PAGE in subfigure (c). (**h**): HPLC RP-C18 chromatogram showing purification of cQ2(PS)-MMAE. Peak 8 was analysed by native PAGE in subfigure (d). Data is representative of multiple repeated experiments.

rHA-Q2/cQ2-Cy5.5 was produced employing different combinations of Q2(DNA), Q2 (i.e. with LNA and 2'-O-Me modifications), cQ2(DNA), cQ2 (LNA and 2'-O-Me modifications), and cQ2(PS) (PS modification in addition to LNA and 2'-O-Me) and stability investigated in 50% FBS at 37°C. Assembly stability was quantified by rHA-associated Cy5.5 fluorescence by native PAGE. This revealed that the Q2(DNA)/cQ2(DNA) homoduplex was almost completely degraded within 24 h, while incorporation of a single strand with stabilised nucleotides greatly improved serum stability (Figure 5). The greatest stability was achieved with Q2/cQ2(PS), where 85% of the annealed conjugate remained intact after 72 h. For this reason, the rHA-Q2/cQ2(PS) assembly was selected for subsequent cellular functional evaluation.

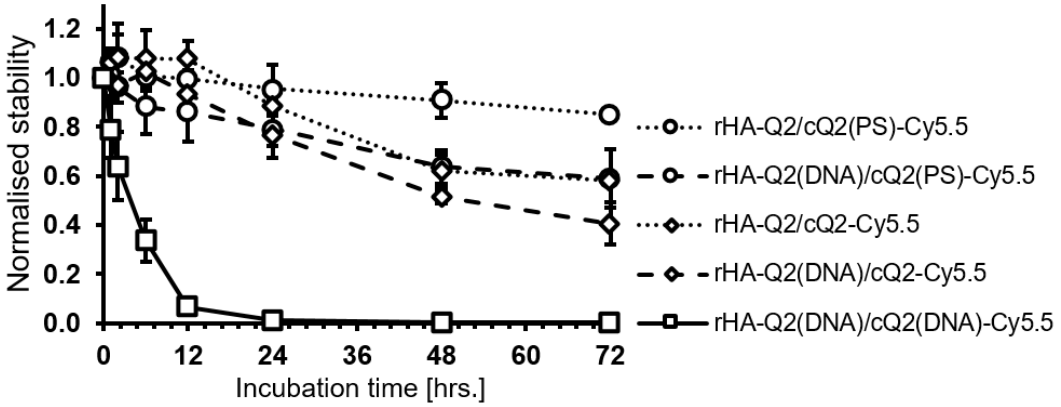

Figure 5. Serum stability of albumin-nucleic acid assemblies. Stability data is based on the Cy5.5 fluorescence signal of rHA-Q2/cQ2-Cy5.5 with different combinations of Q2(DNA), Q2, cQ2(DNA) cQ2, and cQ2(PS) normalised to 0 h. N=2 independent experiments, error bars indicate SEM.

2.3. Cellular functional characterisation of albumin-nucleic acid assemblies

FcRn-mediated cellular recycling was assessed for rHA and the rHA-nucleic acid assemblies (Figure 6). 55.1 pM rHA was recycled in the assay in accordance with previously published work [5], while both rHA-nucleic acid assemblies underwent FcRn-mediated recycling to an even higher degree than rHA alone.

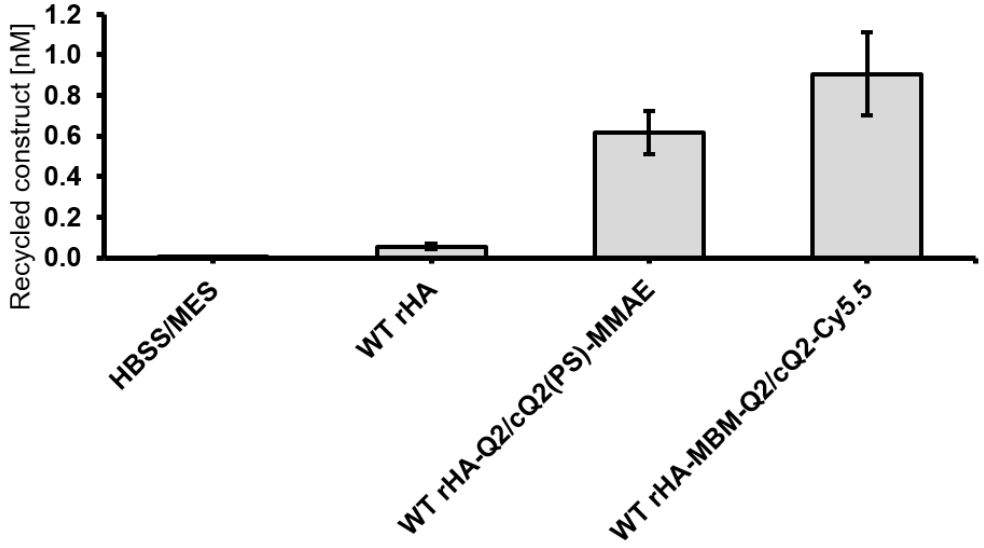

Figure 6. FcRn-mediated cellular recycling assay. ELISA detection of rHA and rHA-nucleic acid conjugate following FcRn-mediated cellular recycling in HMEC-1 FcRn expressing cells. HBSS/MES is a buffer control without any protein. N=4 independent experiments, error bars indicate SEM.

A cell-killing assay was performed in MIA PaCa-2 pancreatic cancer cells to investigate cytotoxic drug efficacy with the biomolecular assembly. While the rHA-Q2 control showed no cell killing over the investigated concentration range, toxicity of the MMAE-azide was observed with an IC50 of 79.9 nM (Figure 7). The stabilised biomolecular assembly employing LNA, 2'-O-Me, and PS oligonucleotides (rHA-Q2/cQ2(PS)-MMAE) exhibited lower toxicity with an IC50 of 342 nM. This is most likely due to steric effects from conjugation of the drug to the oligonucleotide and albumin in addition to the high stability of the LNA, which decreases possible contribution by release of free MMAE through oligonucleotide degradation, and relies exclusively on drug release through cleavage of the acid-labile linker. In accordance with this, toxicity

similar to that of MMAE-azide was observed for the unstabilised rHA-Q2(DNA)/cQ2(DNA)-MMAE construct probably due to the contribution by free drug release through oligonucleotide degradation (data not shown).

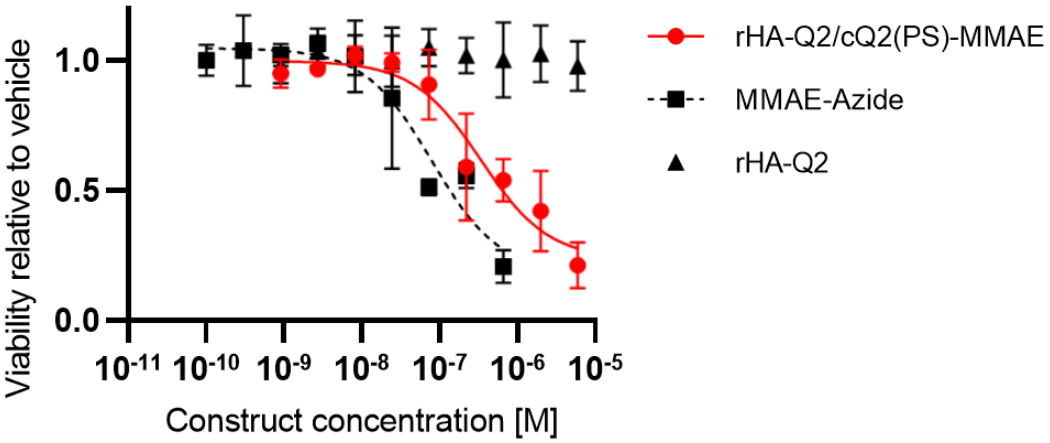

Figure 7. Cell-killing assay. Cell viability determined by MTT assay in MIA PaCa-2 cells after incubation with rHA-Q2/cQ2(PS)-MMAE for 48 h and plotted relative to vehicle (annealing buffer). MMAE-azide: N=2 and the remaining samples N=3 independent experiments, error bars indicate SEM.

3. Discussion

Albumin biomolecular assemblies that utilise nucleic acid scaffolds constitute modular systems to add functionality and maximise drug efficacy. These assemblies offer the potential to multifunctionalise with multiple cytotoxic drugs or include active targeting or imaging modalities for theranostic approaches.

This work aims to improve the translational potential of albumin-nucleic acid assemblies by increasing the stability of the maleimide thiol conjugation and incorporated nucleic acids by employing an MBM linker and modified oligonucleotides, respectively.

The MBM-BCN linker was shown to rapidly conjugate to rHA, and in MS analysis the mass of the Cys34-containing precursor peptide had an increased mass corresponding to the hydrolysed MBM-BCN linker with an oxidised BCN group. Peptide fragmentation allowed determination of the exact conjugation site as being Cys34. After conjugation of the MBM-BCN linker alone to rHA, stabilising hydrolysis proceeded under mild conditions (pH 8.0 at 37°C for 5 h) without any release of conjugated cargo through the retro-Michael reaction. Hydrolysis is required after conjugation to prevent thiol exchange and consequent cargo transfer to other thiol-containing species present in blood (e.g. native serum albumin, cysteines, homocysteine, and glutathione) [18]. However, Cys34 of albumin lies in a ~10 Å deep hydrophobic crevice [6] discommoding hydrolysis [18]. The design of the MBM-BCN-linker has, therefore, been optimised to facilitate the hydrolysis in this region by inclusion of an electron withdrawing C-2 spacer allowing hydrolysis within few hours under mild conditions (pH 8.0 at 37°C) [25]. This is in contrast to the harsher conditions (pH >9 at 37°C overnight) needed for hydrolysis of standard maleimide [25] that can be problematic for payloads such as proteins, peptides, or small molecules susceptible to aggregation at high pH [32, 33]; and can also lead to loss of drug payload during the hydrolysis step [22]. Thus, the rapid reaction speed in combination with hydrolysis under mild conditions with no loss of payload makes MBM-based linkers ideal for production of various biomolecular assemblies.

The free BCN handle of the MBM-BCN linker after conjugation to albumin was utilised for conjugation of a stabilised oligonucleotide. Functionalised complementary oligonucleotides could be efficiently annealed, forming functional albumin-nucleic acid assemblies.

The stability of the albumin-nucleic acid assemblies was investigated in 50% serum, where increased stability was shown by employing LNA-, 2'-O-Me-, and PS-modified oligonucleotides compared to DNA.

Rapid degradation of unmodified nucleic acids by nucleases has been a major factor limiting *in vivo* use of nucleic acids [34]. This has led to a wide range of nucleotide modifications such as the PS [30], 2'-O-Me [29], and LNA [27, 28] that have been used in this work, which all prevent degradation through endo- and exonuclease recognition while the 2'-O-Me and LNA modifications also increase the duplex melting temperature.

Duplex denaturation and nuclease digestion can both result in breakdown of the annealed conjugate. The theoretical melting temperature of the DNA homoduplex used in this work is 54°C [35] affording stability at physiological temperature, thereby, suggesting nuclease digestion to be the major mode of degradation.

FcRn-mediated recycling is the predominant driving force of albumin's extended circulation *in vivo* [36] and has been utilised to extend the circulatory half-life of albumin drug designs [37]. Albumin's Cys34 is located distant from the main FcRn interaction interface, so site-selective conjugation at this site should maintain FcRn engagement. To this end, this work shown the FcRn-engagement was retained for rHA-assemblies functionalised with both Cy5.5 and MMAE in a cellular recycling assay in human endothelial HMEC-1 cells. The *in vitro* FcRn cellular recycling assay has previously been shown to be a good predictor of circulatory half-life performance of albumin drug designs *in vivo* [37, 38] which promotes the albumin-nucleic acid assemblies for drug half-life extension applications.

Interestingly, increased cellular recycling was observed for both functionalised biomolecular assemblies, suggesting some additional mechanism to either increase the amount of endocytosis, exocytosis, or both. It is known that stabilising oligonucleotide modifications can facilitate uptake of oligonucleotides [39], and this could in turn lead to increased FcRn-mediated recycling.

MMAE has been explored as a cytotoxic agent against cancer but, due to its extreme potency and low solubility, requires modification for successful delivery [40]. Association of MMAE to albumin could, therefore, potentially improve its therapeutic performance.

The cytotoxicity of the rHA-nucleic acid assembly functionalised with MMAE was shown with an IC50 of 342 nM. Conjugation of MMAE to cQ2 and annealing of cQ2-MMAE to rHA should both improve the drug's solubility and lower the toxicity compared to MMAE-azide alone, likely by decreased membrane permeability and steric hindrance effects. Importantly, our laboratory has recently shown that FcRn is overexpressed in cancerous tissue in several cancer types, and that FcRn engagement leads to increased albumin accumulation at the tumour site [41], meaning attachment to albumin may potentially mediate targeting of the MMAE construct to cancer tissue. Inclusion of an acid-sensitive linker in the design may allow MMAE release at the low endosomal pH during cellular recycling [42], or low pH environment found in cancer tissue [43].

The drug to albumin ratio (DAR) could be further increased by conjugation to surface lysine residues, but this can lead to heterogeneous drug loading and potential interference with the FcRn binding interface [44, 45]. Utilising a recently developed triple thiol rHA [46] or inclusion of more elaborate nucleic acid scaffolds with multiple handles for conjugation could offer increased DAR with retained site-selective Cys34 conjugation. In the future, this facilitates assemblies with programmable toxicity and supports the possibility for

conjugation of other functionalities such as targeting moieties, while maintaining the FcRn interaction, together contributing to improved cancer therapy.

In this work, an albumin-nucleic acid modular-based conjugate exhibited stability, FcRn-driven cellular recycling, and cancer cell toxicity that promotes its use for future *in vivo* applications.

4. Materials and methods

4.1. Materials

Recombinant human albumin (rHA) expressed in *Saccharomyces cerevisiae* was obtained from Sigma Aldrich (cat# A6608).

The oligonucleotides used in this work are listed in Table 1. DNA oligonucleotides were purchased from Integrated DNA Technologies (Leuven, Belgium). Modified oligonucleotides were synthesised by Jesper Wengel, University of Southern Denmark.

Table 1. Oligonucleotides used for conjugation. Black = DNA, Blue = 2'-O-Me, Red = LNA, * = PS bond, TEG = C_9 spacer.

Oligo name	5' modification	Sequence (5'-3')
Q2(DNA)	NH_2-C_6	CAC AGT GGA CGG
cQ2(DNA)	NH_2-C_6	CCG TCC ACT GTG
Q2	NH_2-C_6	CAC AGT GGA CGG
cQ2	NH_2-C_6-TEG	CCG TCC ACT GTG
cQ2(PS)	NH_2-C_6-TEG	C*C*G* T*C*C* A*C*T* G*T*G

4.2. Synthesis of MBM-BCN linker

The synthesis of MBM-BCN is described in the supporting information.

4.3. Synthesis of MMAE-azide synthesis

The synthesis of MMAE-azide is described in the supporting information.

4.4. Cell lines and cell culture

All cells were cultured at 37°C, 5% CO_2. MIA PaCa-2 cells (ATCC, cat# CRL-1420) in Dulbecco's modified eagle medium (DMEM, Gibco cat# 41965-039) supplemented with 10% fetal bovine serum (FBS), Gibco, cat# 10500-064) and 1% penicillin/streptomycin (P/S) (Gibco, cat# 14140-122). FcRn-transduced human microvascular endothelial cell line-1 (HMEC-1-FcRn) cells were previously generated [5] and cultured in MCDB 131 medium (Life Technologies, cat# 10372-019) with 10 ng/mL human epidermal growth factor (Peprotech, cat# AF-100-15), 1 µg/mL hydrocortisone (Sigma, cat# H0888), 50 µg/mL Geneticin (Gibco, cat# 10131-035), 0.25 µg/mL Puromycin (Life Technologies, cat# A11138-03), 2 mM L-glutamine (Lonza, cat# BE17-605E), and 10% FBS. The cells were used between passage number 20 and 30.

4.5. NanoLC-MS/MS analysis of rHA-MBM-BCN conjugate

rHA was conjugated to the MBM-BCN linker alone (section 4.7) and then trypsin digested as follows: Cold acetone was added in 6-fold volume excess to the rHA-MBM-BCN conjugate and incubated overnight. After centrifugation the rHA pellet was aspirated, dried, and resuspended in 100 µL of 100 mM triethyl ammonium bicarbonate (TEAB) and 5 µL of 200 mM tris(2-carboxyethyl)phosphine (TCEP) and incubated at

55°C for 1 h to reduce cysteine residues. 5 µL of 375 mM iodoacetamide in TEAB was added and incubated for 30 min at room temperature (RT) to block cysteines. 2.5 µg trypsin was then added per 100 µg rHA-MBM-BCN conjugate for digestion overnight at 37°C with 400 rpm orbital shaking.

The peptides were purified with a C18 centrifugation column before nano-liquid chromatography-tandem mass spectrometry (nanoLC-MS/MS) analysis using an EASY nanoLC-1000 (Thermo Scientific) coupled to Q Exactive™ HF-X Hybrid Quadrupole-Orbitrap™ Mass Spectrometer (Thermo Fisher Scientific). The peptides were trapped on a pre-column (PepMap 100, 2 cm, 75 µm i.d., 3 µm C18 particles, 100 Å, Thermo Scientific) followed by reverse-phase separation on a C18 column with integrated emitter (EASY-Spray column, PepMap 25 cm, 75 µm i.d., 2 µm, 100 Å, Thermo Scientific). The peptides were separated in a 45 min linear gradient, from 4 to 40% acetonitrile in 0.1% formic acid at a flow rate of 300 nL/min. The MS was operated in a positive, data-dependent mode, automatically switching between precursor scanning (MS1) and fragmentation (MS2) acquisition. Resolution of MS1 was set to 60,000 and MS2 to 15,000. Up to ten of the most intense ions were fragmented (MS2) per every MS1 scan, by higher-energy C-trap dissociation (HCD).

Data from nanoLC-MS/MS were searched against an in house created database containing the human proteome (20,151 human proteins from Uniprot) including rHA. Identification based on peptide mass and peptide fragmentation pattern and was performed in Proteome Discoverer 2.3 (Thermo Fisher Scientific) using the Sequest algorithm. In the search, the possibility for 511.22 Da modification on cysteine (corresponding to the mass of the conjugated and hydrolysed MBM-BCN linker with oxidised BCN) was included.

4.6. UV-Vis measurements of rHA-MBM-BCN conjugate reaction and hydrolysis kinetics

An Evolution 260 Bio UV-Visible spectrophotometer (Thermo Scientific) was used for absorbance measurement in quartz cuvettes with a 1 cm path length. Samples were baseline corrected.

MBM-BCN linker (100 nmol, 5.0 eq.) in 10 µL dimethylsulfoxid (DMSO, Sigma, cat# 276855) was conjugated to rHA (20 nmol, 1.0 eq.), diluted to 200 µL with 0.1 M 4-(2-hydroxyethyl)-1-piperazineethanesulfonic acid (HEPES, Sigma, cat# H4034) pH 7.0, incubating at 20°C. Absorbance measurement at 350 nm indicates thiomaleimide formation [25].

Hydrolysis was performed by adding 0.1 M HEPES pH 8.0 in a 9-fold volume excess and incubating at 37°C. Decreasing absorbance at 350 nm indicates ring-opening of the thiomaleimide by hydrolysis [25].

Data analysis was performed in GraphPad Prism (version 9.2.0) using a one-phase association model with Y_0 constrained to 0 or 1 for the normalised 350 nm absorbance measurement of the reaction or hydrolysis data, respectively.

4.7. MBM-BCN conjugation to rHA and attachment of oligonucleotide

MBM-BCN linker (100 nmol, 5.0 eq.) in DMSO (10 µL) was conjugated to rHA (20 nmol, 1.0 eq.), diluted to 200 µL with 0.1 M HEPES pH 7.0 by incubating for 15 min at RT with 650 rpm orbital shaking. Excess linker was removed by spin filtration through a 10 kDa molecular weight cut-off membrane filter (Merck, cat# UFC501096). The BCN-modified rHA (~20 nmol, 1.0 eq.) in 0.1 M HEPES pH 7.0 (~35 µL) was conjugated to 10 nmol (~0.5 eq.) tetrazine-modified Cy5.5 (Lumiprobe, cat# 170E0) in DMSO (1 µL) or tetrazine-modified oligonucleotide (section 4.8) in nuclease-free water (NFW, Invitrogen, cat# AM9937) (20 µL) overnight at RT with 650 rpm orbital shaking.

The rHA-oligonucleotide conjugate was hydrolysed by adding 0.1 M HEPES pH 8.0 in a 9-fold volume excess and incubating at 37°C for at least 6 h with 650 rpm orbital shaking.

The rHA-oligonucleotide conjugate was purified with high-performance liquid chromatography (HPLC) using an ion-exchange (IEX) column (section 4.9) resulting in yields of >40% with respect to the starting amount of oligonucleotide.

4.8. Oligonucleotide functionalisation

Q2-Tetrazine

Tetrazine-$(PEG)_5$-NHS-ester linker (BroadPharm, cat# BP-22681, Figure S3) (500 nmol, 50 eq.) in DMSO (5 µL) was conjugated to Q2 oligonucleotide (10 nmol, 1.0 eq.) in NFW (10 µL) with 15 µL DMSO and 30 µL 0.1 M HEPES pH 8.0 incubating overnight at RT with 650 rpm orbital shaking. Excess linker was removed by ethanol precipitation (described below).

cQ2-Cy5.5

Cy5.5-NHS-ester linker (Lumiprobe, cat# 47020) (100 nmol, 20 eq.) in DMSO (10 µL) was conjugated to cQ2 oligonucleotide (5 nmol, 1.0 eq.) in NFW (5 µL) with 10 µL DMSO and 35 µL 0.1 M HEPES pH 8.0 incubating overnight at RT with 650 rpm orbital shaking. Excess linker was removed by ethanol precipitation (described below) and the conjugate was purified with using with HPLC using a reversed-phase (RP) column (section 4.9).

cQ2-MMAE

NHS-ester-dibenzocyclooctyne (DBCO) linker (Sigma, cat# 761524) (200 nmol, 20 eq.) in DMSO (2 µL) was conjugated to cQ2 oligonucleotide (10 nmol, 1.0 eq.) in NFW (10 µL) with 30 µL DMSO and 70 µL 0.1 M HEPES pH 8.0 incubating overnight at RT with 650 rpm orbital shaking. Excess linker was removed by ethanol precipitation (described below). The cQ2-DBCO in NFW (20 µL) was then conjugated to MMAE-azide (section 4.3) (20 nmol, ~2 eq.) in DMSO (10 µL) by incubating overnight at RT with 650 rpm orbital shaking. Next, the conjugate was purified with HPLC using an RP column (section 4.9).

Ethanol precipitation of oligonucleotide conjugates

Oligonucleotide (1.25 vol. eq.), absolute ethanol (EtOH, VWR, cat# 20821.310) (7.75 vol. eq.), and 3 M sodium acetate (NaOAc, Sigma, cat# S2889) (1.00 vol. eq.) was mixed and incubated at -18°C for 2.5-3 h followed by centrifugation (17,000 g, 45 min). The pellet was aspirated, washed with EtOH, and centrifuged (17,000 g, 30 min). The pellet was dried for 10 min and dissolved in NFW or 0.1 M HEPES pH 7.0.

LC-MS confirmation of conjugation

LC-MS was used for confirmation of functionalised oligonucleotide masses as described in [47].

4.9. Preparative and analytical HPLC

The HPLC system consists of a low pressure gradient (LPG)-3400RS pump, a variable wavelength detector (VWD)-3400RS, and Ultimate 3000 automated fraction collector (AFC, all from Thermo Fisher Scientific). Samples were loaded using a 100 µL Hamilton syringe (Sigma-Aldrich) into a Rheodyne 9725i manual injector (Thermo Fisher Scientific) connected to a 500 µL polyether ether ketone (PEEK) sample loop. Samples were filtered with a 0.2 µm polypropylene (PP) filter (Kinesis, cat# ESF-PP-04-022) before injection on the HPLC.

Preparative IEX chromatography

IEX chromatography was performed with a Mono Q 5/50 GL anion exchange column (Cytiva) with the following program at 0.3 mL/min: 5 min buffer A (20 mM Tris (Sigma, cat# T5941) and 10 mM NaCl (Acros Organics, cat# 207790010) at pH 7.6), a 25 min gradient to buffer B (20 mM Tris and 800 mM NaCl at pH 7.6), 5 min of buffer B, a 5 min gradient to buffer A and finally 5 min of buffer A. Absorbance was measured

at 224 and 260 nm. The collected fractions were desalted and concentrated by centrifugation through 10 or 30 kDa molecular weight cut-off membrane filters.

Preparative RP chromatography

Preparative RP chromatography was performed with an XTerra MS C18 column (Waters) with the following program at 0.5 mL/min: 2.5-5 min buffer A (5% triethylammonium acetate (TEAA), Sigma, cat# 69372) and 5% acetonitrile (MeCN, VWR, cat# 83639.320) in MilliQ water), a 17.5-20 min gradient to buffer B (100% MeCN), 5 min of buffer B, a 2.5-5 min gradient to buffer A, and lastly 2.5-5 min buffer A. Absorbance was measured at 260 and 684 nm. The solvent of the collected fractions was evaporated using a RVC 2-18 speed vacuum centrifuge (Martin Christ) and resuspended in NFW.

Analytical RP chromatography

Analytical RP chromatography was performed with a PerfectSil 300 C4 column (MZ Analytical) running the following program at 0.7 mL/min: 5 min buffer A (0.1% trifluoroacetic acid (TFA, Sigma cat# T6508) in MilliQ water), a 5 min gradient to 35% buffer B (75% isopropanol (VWR, cat# 20880.320) in MilliQ water), a 25 min gradient to 60% buffer B, a 4 min gradient to 95% buffer B, 6 min of buffer B, a 5 min gradient to buffer A and lastly 5 min buffer A. Absorbance was measured at 280 and 684 nm.

4.10. Annealing of functionalised oligonucleotides

For oligonucleotide annealing, complementary strands were added in equimolar amounts to a concentration of 200 mM potassium acetate (KOAc, Sigma, cat# P1190). The solution was heated to 55-60°C and slowly cooled to RT over 1.5-2 h.

Oligonucleotide concentration was determined by absorbance at 260 nm, if necessary compensating for fluorophore absorbance (Cy5.5 260 nm correction factor (CF_{260}) is 0.07). rHA-nucleic acid conjugate concentration was determined using a bicinchoninic acid (BCA) assay (Thermo Scientific, cat# 23225) according to the manufacturer's protocol.

4.11. Gel electrophoresis of functionalised oligonucleotides and biomolecular assemblies

Casting of 15% native PAGE gels: 5 mL ProtoGel (National Diagnostics, cat# EC-890), 4 mL MilliQ water, 1 mL 10X tris, borate, ethylenediamine tetraacetic acid (TBE, Thermo Fisher Scientific, cat# 15581-044), 100 µL 10% ammonium persulfate (APS, Sigma, cat# A3678), and 10 µL *N*,*N*,*N*',*N*'-tetramethylethylenediamine (TEMED, Sigma, cat# T9281) were mixed, poured into 1 mm cassettes (Invitrogen, cat# NC2010), a 10 or 12-well comb (Invitrogen cat# NC3010 or NC3012) inserted, and gels polymerised for 45 min.

Native PAGE samples were mixed with loading buffer to 10% glycerol (VWR, cat# 24388.295) and 1 g/L Orange G (Sigma, cat# O3756) and loaded in a gel run using TBE running buffer. Gels were run at 125-150 V for 75-120 min at RT with an EPS 601 electrophoresis power supply (Amersham Biosciences).

SYBR Gold (Invitrogen, cat# S11494) staining was performed using 1X SYBR Gold in MilliQ for 15 min. SYBR Gold and conjugated fluorophores were imaged on an Amersham Typhoon 5 (Cytiva).

4.12. Serum stability assay of biomolecular assemblies

rHA-Q2/cQ2-Cy5.5 conjugates were incubated in 50% FBS in PBS at 37°C. Samples were stored at -18°C after 0, 1, 2, 6, 12, 24, 48, and 72 h, and subsequently analysed by native PAGE using the Cy5.5 fluorescence signal to quantify the intact conjugate.

4.13. FcRn-mediated cellular recycling assay of biomolecular assemblies

The FcRn-mediated cellular recycling assay was performed according to Schmidt *et al*. [5]. 100,000 HMEC-1-FcRn cells were seeded in a 48-well plate (Sarstedt, cat# 83.3923) coated with 100 µL of 1:30 GelTrex (Life Technologies, cat# A1413202) for 1 h at 37°C and incubated until near confluent. HMEC-1-FcRn cells were washed twice with warm PBS before incubation with 300 µL analyte (150.4 nM analyte in Hank's Balanced Salt Solution (Sigma, cat# H9269) adjusted to pH 6.0 with MES buffer (Sigma, cat# M1317)) for 1 h at RT. Cells were washed with 4°C PBS, before incubation with 160 µL serum-free medium for 1 h. The supernatant was harvested and the amount of recycled analyte was quantified by sandwich ELISA:

96-well plates were coated with anti-albumin capture antibody (Sigma, cat# A7544) 1:1000 in PBS for 2 h at RT, blocked with 2% mPBS for 2 h at RT, and washed with 0.05% PBST before incubation overnight at 4°C with recycling samples and standard of the corresponding analytes. Wells were washed, incubated for 2 h at RT with HRP-conjugated anti-albumin antibody (Abcam, cat# ab8941, diluted 1:5000 in 2% mPBS), washed again, and TMB was added. The reaction was stopped with 0.2 M H_2SO_4, and the absorbance at 450 nm was measured using a Clariostar plate reader with background subtraction of the absorbance at 655 nm. The data was analysed using GraphPad Prism 9.2.0.

4.14. Cell killing assay of MMAE-functionalised biomolecular assembly

7,500 MIA PaCa-2 cells were seeded in a 96-well plate (Sarstedt, cat # 83.3924) previously coated with 50 µL of 1:50 GelTrex for 1 h at 37°C. After 24 h, wells were aspirated, and the cells were incubated with medium containing analyte for 48 h.

3-(4,5-dimethylthiazol-2-yl)-2,5-diphenyltetrazolium bromide (MTT) assay (Roche, cat# 11 465 007 001) was performed according to the manufacturer's protocol. Cells were incubated with the MTT reagent for 30-45 min and absorbance was measured at 570 nm (data) and 690 nm (background) using a Clariostar plate reader. Data was analysed using a four-parameter logistic curve in Graphpad Prism 9.2.0.

5. Associated content

Supporting Information: Monobromomaleimide reaction with albumin, MBM-BCN linker hydrolysis stability, chemical structure of Tetrazine-(PEG)5-NHS-ester linker, and description of synthesis of MBM-BCN and MMAE-azide linkers.

6. Acknowledgements

This research was funded by the Novo Nordisk Foundation, Grant; CEMBID (Center for Multifunctional Biomolecular Drug Design, Grant Number: NNF17OC0028070) and the Villum Fonden, Grant; BioNEC (Biomolecular Nanoscale Engineering Center, Grant Number: VKR18333).

7. Abbreviations

2'-O-methyl (2'-O-Me), 260 nm correction factor (CF260), 3-(4,5-dimethylthiazol-2-yl)-2,5-diphenyltetrazolium bromide (MTT) assay, 4-(2-hydroxyethyl)-1-piperazineethanesulfonic acid (HEPES), acetonitrile (MeCN), ammonium persulfate (APS), antibody-drug conjugates (ADCs), bicinchoninic acid (BCA), bicyclo[6.1.0]nonyne (BCN), CEMBID (Center for Multifunctional Biomolecular Drug Design, cysteine 34 (Cys34), dibenzocyclooctyne (DBCO), dimethylsulfoxid (DMSO), drug to albumin ratio (DAR), Dulbecco's modified eagle medium (DMEM), ethanol (EtOH), FcRn-transduced human microvascular endothelial cell line-1 (HMEC-1-FcRn), higher-energy C-trap dissociation (HCD), high-performance liquid chromatography (HPLC), ion-exchange (IEX), locked nucleic acid (LNA), low pressure gradient (LPG), monobromomaleimide

(MBM), monomethyl auristatin E (MMAE), *N*,*N*,*N'*,*N'*-tetramethylethylenediamine (TEMED), nano-liquid chromatography-tandem mass spectrometry (nanoLC-MS/MS), neonatal Fc receptor (FcRn), nuclease-free water (NFW), penicillin/streptomycin (P/S), phosphorothioate (PS), poly(ethylene glycol) (PEG), polyether ether ketone (PEEK), polypropylene (PP), potassium acetate (KOAc), recombinant human albumin (rHA), reversed-phase (RP), room temperature (RT), sodium acetate (NaOAc), triethyl ammonium bicarbonate (TEAB), triethylammonium acetate (TEAA), trifluoroacetic acid (TFA), tris(2-carboxyethyl)phosphine (TCEP), tris, borate, ethylenediamine tetraacetic acid (TBE), variable wavelength detector (VWD).

Conflicts of Interest: The authors declare no competing financial interest.

8. References

1. Markovsky, E.; Baabur-Cohen, H.; Eldar-Boock, A.; Omer, L.; Tiram, G.; Ferber, S.; Ofek, P.; Polyak, D.; Scomparin, A.; Satchi-Fainaro, R., Administration, distribution, metabolism and elimination of polymer therapeutics. *Journal of controlled release : official journal of the Controlled Release Society* **2012,** *161* (2), 446-60.
2. Sleep, D.; Cameron, J.; Evans, L. R., Albumin as a versatile platform for drug half-life extension. *Biochimica et biophysica acta* **2013,** *1830* (12), 5526-34.
3. Abuchowski, A.; van Es, T.; Palczuk, N. C.; Davis, F. F., Alteration of immunological properties of bovine serum albumin by covalent attachment of polyethylene glycol. *The Journal of biological chemistry* **1977,** *252* (11), 3578-81.
4. Szlachcic, A.; Zakrzewska, M.; Otlewski, J., Longer action means better drug: tuning up protein therapeutics. *Biotechnology advances* **2011,** *29* (4), 436-41.
5. Schmidt, E. G. W.; Hvam, M. L.; Antunes, F.; Cameron, J.; Viuff, D.; Andersen, B.; Kristensen, N. N.; Howard, K. A., Direct demonstration of a neonatal Fc receptor (FcRn)-driven endosomal sorting pathway for cellular recycling of albumin. *The Journal of biological chemistry* **2017,** *292* (32), 13312-13322.
6. Pilati, D.; Howard, K. A., Albumin-based drug designs for pharmacokinetic modulation. *Expert Opinion on Drug Metabolism & Toxicology* **2020,** *16* (9), 783-795.
7. Larsen, M. T.; Kuhlmann, M.; Hvam, M. L.; Howard, K. A., Albumin-based drug delivery: harnessing nature to cure disease. *Molecular and cellular therapies* **2016,** *4*, 3.
8. Petersen, S. S.; Kläning, E.; Ebbesen, M. F.; Andersen, B.; Cameron, J.; Sørensen, E. S.; Howard, K. A., Neonatal Fc Receptor Binding Tolerance toward the Covalent Conjugation of Payloads to Cysteine 34 of Human Albumin Variants. *Molecular pharmaceutics* **2016,** *13* (2), 677-82.
9. Bednar, R. A., Reactivity and pH dependence of thiol conjugation to N-ethylmaleimide: detection of a conformational change in chalcone isomerase. *Biochemistry* **1990,** *29* (15), 3684-3690.
10. Frayne, S. H.; Murthy, R. R.; Northrop, B. H., Investigation and Demonstration of Catalyst/Initiator-Driven Selectivity in Thiol-Michael Reactions. *The Journal of Organic Chemistry* **2017,** *82* (15), 7946-7956.
11. Chan, J. W.; Hoyle, C. E.; Lowe, A. B.; Bowman, M., Nucleophile-Initiated Thiol-Michael Reactions: Effect of Organocatalyst, Thiol, and Ene. *Macromolecules* **2010,** *43* (15), 6381-6388.
12. Nair, D. P.; Podgórski, M.; Chatani, S.; Gong, T.; Xi, W.; Fenoli, C. R.; Bowman, C. N., The Thiol-Michael Addition Click Reaction: A Powerful and Widely Used Tool in Materials Chemistry. *Chemistry of Materials* **2014,** *26* (1), 724-744.
13. Nejadmoghaddam, M. R.; Minai-Tehrani, A.; Ghahremanzadeh, R.; Mahmoudi, M.; Dinarvand, R.; Zarnani, A. H., Antibody-Drug Conjugates: Possibilities and Challenges. *Avicenna journal of medical biotechnology* **2019,** *11* (1), 3-23.
14. Jain, N.; Smith, S. W.; Ghone, S.; Tomczuk, B., Current ADC Linker Chemistry. *Pharmaceutical research* **2015,** *32* (11), 3526-40.
15. Kratz, F., Albumin as a drug carrier: Design of prodrugs, drug conjugates and nanoparticles. *Journal of Controlled Release* **2008,** *132* (3), 171-183.
16. Fontaine, S. D.; Reid, R.; Robinson, L.; Ashley, G. W.; Santi, D. V., Long-Term Stabilization of Maleimide–Thiol Conjugates. *Bioconjugate Chemistry* **2015,** *26* (1), 145-152.
17. Ponte, J. F.; Sun, X.; Yoder, N. C.; Fishkin, N.; Laleau, R.; Coccia, J.; Lanieri, L.; Bogalhas, M.; Wang, L.; Wilhelm, S.; Widdison, W.; Pinkas, J.; Keating, T. A.; Chari, R.; Erickson, H. K.; Lambert, J. M., Understanding How the Stability of the Thiol-Maleimide Linkage Impacts the Pharmacokinetics of Lysine-Linked Antibody-Maytansinoid Conjugates. *Bioconjug Chem* **2016,** *27* (7), 1588-98.
18. Shen, B.-Q.; Xu, K.; Liu, L.; Raab, H.; Bhakta, S.; Kenrick, M.; Parsons-Reponte, K. L.; Tien, J.; Yu, S.-F.; Mai, E.; Li, D.; Tibbitts, J.; Baudys, J.; Saad, O. M.; Scales, S. J.; McDonald, P. J.; Hass, P. E.; Eigenbrot, C.; Nguyen, T.; Solis, W. A.; Fuji, R. N.; Flagella, K. M.; Patel, D.; Spencer, S. D.; Khawli, L. A.; Ebens, A.; Wong, W. L.; Vandlen, R.; Kaur, S.; Sliwkowski, M. X.; Scheller, R. H.; Polakis, P.; Junutula, J. R.,

Conjugation site modulates the in vivo stability and therapeutic activity of antibody-drug conjugates. *Nature biotechnology* **2012,** *30* (2), 184-189.
19. Jackson, D.; Atkinson, J.; Guevara, C. I.; Zhang, C.; Kery, V.; Moon, S. J.; Virata, C.; Yang, P.; Lowe, C.; Pinkstaff, J.; Cho, H.; Knudsen, N.; Manibusan, A.; Tian, F.; Sun, Y.; Lu, Y.; Sellers, A.; Jia, X. C.; Joseph, I.; Anand, B.; Morrison, K.; Pereira, D. S.; Stover, D., In vitro and in vivo evaluation of cysteine and site specific conjugated herceptin antibody-drug conjugates. *PloS one* **2014,** *9* (1), e83865.
20. Caspersen, M. B.; Kuhlmann, M.; Nicholls, K.; Saxton, M. J.; Andersen, B.; Bunting, K.; Cameron, J.; Howard, K. A., Albumin-based drug delivery using cysteine 34 chemical conjugates - important considerations and requirements. *Therapeutic delivery* **2017,** *8* (7), 511-519.
21. Alley, S. C.; Benjamin, D. R.; Jeffrey, S. C.; Okeley, N. M.; Meyer, D. L.; Sanderson, R. J.; Senter, P. D., Contribution of Linker Stability to the Activities of Anticancer Immunoconjugates. *Bioconjugate Chemistry* **2008,** *19* (3), 759-765.
22. Smith, M. E.; Caspersen, M. B.; Robinson, E.; Morais, M.; Maruani, A.; Nunes, J. P.; Nicholls, K.; Saxton, M. J.; Caddick, S.; Baker, J. R.; Chudasama, V., A platform for efficient, thiol-stable conjugation to albumin's native single accessible cysteine. *Org Biomol Chem* **2015,** *13* (29), 7946-9.
23. Ravasco, J.; Faustino, H.; Trindade, A.; Gois, P. M. P., Bioconjugation with Maleimides: A Useful Tool for Chemical Biology. *Chemistry (Weinheim an der Bergstrasse, Germany)* **2019,** *25* (1), 43-59.
24. Tedaldi, L. M.; Smith, M. E.; Nathani, R. I.; Baker, J. R., Bromomaleimides: new reagents for the selective and reversible modification of cysteine. *Chemical communications (Cambridge, England)* **2009,** (43), 6583-5.
25. Wall, A.; Nicholls, K.; Caspersen, M. B.; Skrivergaard, S.; Howard, K. A.; Karu, K.; Chudasama, V.; Baker, J. R., Optimised approach to albumin–drug conjugates using monobromomaleimide-C-2 linkers. *Organic & Biomolecular Chemistry* **2019,** *17* (34), 7870-7873.
26. Kuhlmann, M.; Hamming, J. B. R.; Voldum, A.; Tsakiridou, G.; Larsen, M. T.; Schmøkel, J. S.; Sohn, E.; Bienk, K.; Schaffert, D.; Sørensen, E. S.; Wengel, J.; Dupont, D. M.; Howard, K. A., An Albumin-Oligonucleotide Assembly for Potential Combinatorial Drug Delivery and Half-Life Extension Applications. *Molecular therapy. Nucleic acids* **2017,** *9*, 284-293.
27. K. Singh, S.; A. Koshkin, A.; Wengel, J.; Nielsen, P., LNA (locked nucleic acids): synthesis and high-affinity nucleic acid recognition. *Chemical Communications* **1998,** (4), 455-456.
28. Obika, S.; Nanbu, D.; Hari, Y.; Andoh, J.-i.; Morio, K.-i.; Doi, T.; Imanishi, T., Stability and structural features of the duplexes containing nucleoside analogues with a fixed N-type conformation, 2′-O,4′-C-methyleneribonucleosides. *Tetrahedron Letters* **1998,** *39* (30), 5401-5404.
29. Inoue, H.; Hayase, Y.; Imura, A.; Iwai, S.; Miura, K.; Ohtsuka, E., Synthesis and hybridization studies on two complementary nona(2'-O-methyl)ribonucleotides. *Nucleic acids research* **1987,** *15* (15), 6131-48.
30. Vosberg, H. P.; Eckstein, F., Effect of deoxynucleoside phosphorothioates incorporated in DNA on cleavage by restriction enzymes. *The Journal of biological chemistry* **1982,** *257* (11), 6595-9.
31. Spangler, B.; Yang, S.; Baxter Rath, C. M.; Reck, F.; Feng, B. Y., A Unified Framework for the Incorporation of Bioorthogonal Compound Exposure Probes within Biological Compartments. *ACS Chemical Biology* **2019,** *14* (4), 725-734.
32. Chi, E. Y.; Krishnan, S.; Randolph, T. W.; Carpenter, J. F., Physical stability of proteins in aqueous solution: mechanism and driving forces in nonnative protein aggregation. *Pharmaceutical research* **2003,** *20* (9), 1325-36.
33. Tian, J.; Stella, V. J., Degradation of Paclitaxel and Related Compounds in Aqueous Solutions II: Nonepimerization Degradation Under Neutral to Basic pH Conditions. *Journal of Pharmaceutical Sciences* **2008,** *97* (8), 3100-3108.
34. Okholm, A. H.; Kjems, J., DNA nanovehicles and the biological barriers. *Adv Drug Deliv Rev* **2016,** *106* (Pt A), 183-191.
35. Owczarzy, R.; Tataurov, A. V.; Wu, Y.; Manthey, J. A.; McQuisten, K. A.; Almabrazi, H. G.; Pedersen, K. F.; Lin, Y.; Garretson, J.; McEntaggart, N. O.; Sailor, C. A.; Dawson, R. B.; Peek, A. S., IDT

SciTools: a suite for analysis and design of nucleic acid oligomers. *Nucleic acids research* **2008,** *36* (Web Server issue), W163-W169.
36. Chaudhury, C.; Mehnaz, S.; Robinson, J. M.; Hayton, W. L.; Pearl, D. K.; Roopenian, D. C.; Anderson, C. L., The major histocompatibility complex-related Fc receptor for IgG (FcRn) binds albumin and prolongs its lifespan. *J Exp Med* **2003,** *197* (3), 315-322.
37. Mandrup, O. A.; Ong, S. C.; Lykkemark, S.; Dinesen, A.; Rudnik-Jansen, I.; Dagnæs-Hansen, N. F.; Andersen, J. T.; Alvarez-Vallina, L.; Howard, K. A., Programmable half-life and anti-tumour effects of bispecific T-cell engager-albumin fusions with tuned FcRn affinity. *Communications Biology* **2021,** *4* (1), 310.
38. Larsen, M. T.; Rawsthorne, H.; Schelde, K. K.; Dagnæs-Hansen, F.; Cameron, J.; Howard, K. A., Cellular recycling-driven in vivo half-life extension using recombinant albumin fusions tuned for neonatal Fc receptor (FcRn) engagement. *Journal of controlled release : official journal of the Controlled Release Society* **2018,** *287*, 132-141.
39. Deprey, K.; Batistatou, N.; Kritzer, J. A., A critical analysis of methods used to investigate the cellular uptake and subcellular localization of RNA therapeutics. *Nucleic acids research* **2020,** *48* (14), 7623-7639.
40. Newman, D. J.; Cragg, G. M., Current Status of Marine-Derived Compounds as Warheads in Anti-Tumor Drug Candidates. *Mar Drugs* **2017,** *15* (4), 99.
41. Larsen, M. T.; Mandrup, O. A.; Schelde, K. K.; Luo, Y.; Sørensen, K. D.; Dagnæs-Hansen, F.; Cameron, J.; Stougaard, M.; Steiniche, T.; Howard, K. A., FcRn overexpression in human cancer drives albumin recycling and cell growth; a mechanistic basis for exploitation in targeted albumin-drug designs. *Journal of Controlled Release* **2020,** *322*, 53-63.
42. Rudnik-Jansen, I.; Howard, K. A., FcRn expression in cancer: Mechanistic basis and therapeutic opportunities. *Journal of Controlled Release* **2021,** *337*, 248-257.
43. Tannock, I. F.; Rotin, D., Acid pH in tumors and its potential for therapeutic exploitation. *Cancer research* **1989,** *49* (16), 4373-84.
44. Di Stefano, G.; Fiume, L.; Baglioni, M.; Bolondi, L.; Chieco, P.; Kratz, F.; Pariali, M.; Rubini, G., Efficacy of doxorubicin coupled to lactosaminated albumin on rat hepatocellular carcinomas evaluated by ultrasound imaging. *Digestive and liver disease : official journal of the Italian Society of Gastroenterology and the Italian Association for the Study of the Liver* **2008,** *40* (4), 278-84.
45. Burger, A. M.; Hartung, G.; Stehle, G.; Sinn, H.; Fiebig, H. H., Pre-clinical evaluation of a methotrexate-albumin conjugate (MTX-HSA) in human tumor xenografts in vivo. *International journal of cancer* **2001,** *92* (5), 718-24.
46. Schelde, K. K.; Nicholls, K.; Dagnæs-Hansen, F.; Bunting, K.; Rawsthorne, H.; Andersen, B.; Finnis, C. J. A.; Williamson, M.; Cameron, J.; Howard, K. A., A new class of recombinant human albumin with multiple surface thiols exhibits stable conjugation and enhanced FcRn binding and blood circulation. *The Journal of biological chemistry* **2019,** *294* (10), 3735-3743.
47. Märcher, A.; Nijenhuis, M. A. D.; Gothelf, K. V., A Wireframe DNA Cube: Antibody Conjugate for Targeted Delivery of Multiple Copies of Monomethyl Auristatin E. *Angewandte Chemie (International ed. in English)* **2021**.
48. Mortensen, M. R.; Skovsgaard, M. B.; Märcher, A.; Andersen, V. L.; Palmfeldt, J.; Nielsen, T. B.; Tørring, T.; Laursen, N. S.; Andersen, K. R.; Kjems, J.; Gothelf, K. V., Introduction of an Aldehyde Handle on Nanobodies by Affinity-Guided Labeling. *Bioconjugate Chemistry* **2020,** *31* (5), 1295-1300.

9. Table of contents graphic

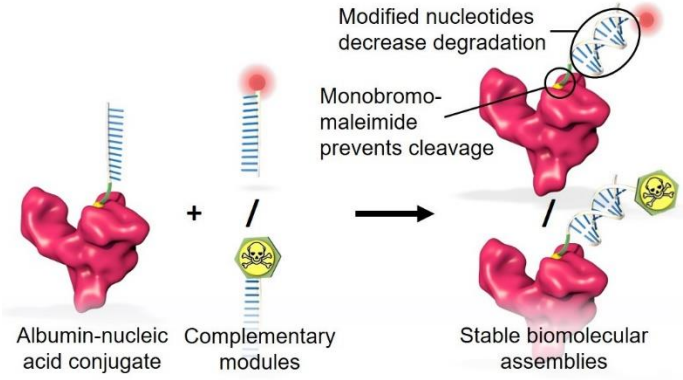

10. Supporting information

10.1. Supporting figures

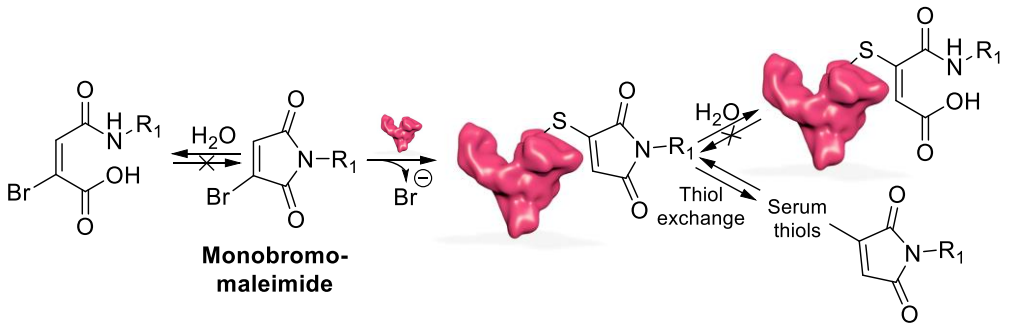

Figure S1. Monobromomaleimide reaction with cysteine 34 on albumin.

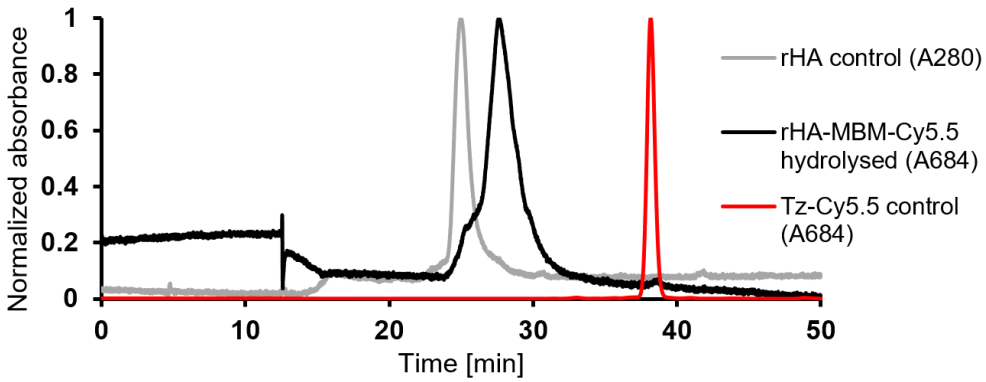

Figure S2. MBM-BCN linker stability after hydrolysis. HPLC-RP of hydrolysed rHA-MBM-fluorophore showing no release of conjugate during hydrolysis.

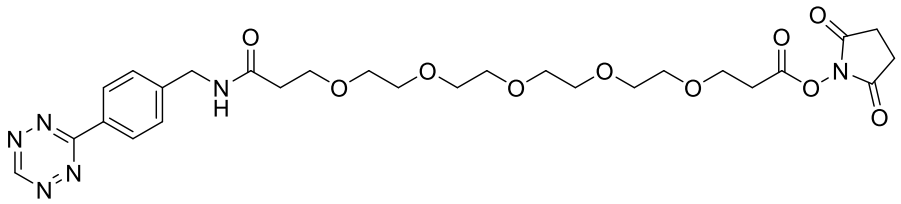

Figure S3. Chemical structure of Tetrazine-$(PEG)_5$-NHS-ester linker.

10.2. Synthesis of MBM-BCN linker

2-(3-bromo-2,5-dioxo-2,5-dihydro-1*H*-pyrrol-1-yl)acetic acid (1)

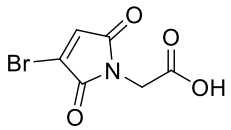

Synthesised as previously reported [25].

MBM-BCN (2)

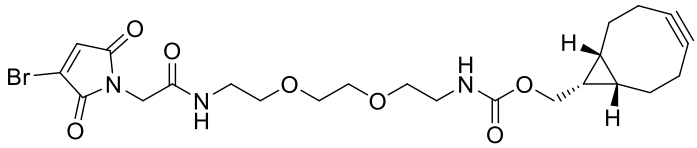

Under an atmosphere of argon, EEDQ (38.6 mg, 0.156 mmol, 1.33 eq.) was added to compound **1** (38.0 mg, 0.162 mmol, 1.38 eq.) dissolved in MeCN (8 mL). The solution was stirred at room temperature for 30 min, before BCN-amine was added (38.0 mg, 0.117 mmol, 1.00 eq. in MeCN (1 mL)). After 1 h, the solvent was removed *in vacuo*, and the crude product purified by flash chromatography (0-100% EtOAc/Hexane, followed by 0-10% MeOH in DCM) to leave a highly viscous brown oil (26.6 mg, 0.049 mmol, 42%).

^{1}H NMR (700 MHz, $CDCl_3$) δ 7.92 (br s, 0.3H, N*H*), 6.98 – 6.90* (m, 1H, C=C*H*), 6.49 (br s, 0.6H, N*H*), 5.84 (br s, 0.3H, N*H*), 5.22 (br s, 0.6H, N*H*), 4.27 – 4.21 (m, 2H, NCH_2), 4.18 – 4.12 (m, 2H, C(O)OCH_2), 3.71 – 3.53 (m, 8H, 4 x OCH_2), 3.46 (q, *J* = 5.3 Hz, 2H, CH_2C(O)NHCH_2), 3.39 – 3.35 (m, 2H, OC(O)NHCH_2), 2.31 – 2.17 (m, 6H, 2 x CCH_2, 2 x CCH_2C*H*H), 1.59-1.54 (m, 2H, 2 x CCH_2CH*H*), 1.40 – 1.30 (m, 1H, OCH_2C*H*), 0.98 – 0.89 (m, 2H, 2 x OCH_2CHC*H*) (Figure S4 and Figure S5). **assigned multiplet due to partially overlapping amide rotamer.*

^{13}C NMR (176 MHz, $CDCl_3$) δ 168.2, 165.7, 165.1, 157.0, 132.4, 131.8, 98.9, 70.5, 70.3, 70.2, 69.7, 63.0, 41.2, 40.9, 39.7, 29.2, 21.5, 20.2, 17.9 (Figure S6). *(Where amide rotamers are present, the highest intensity peak has been assigned).*

IR (oil) V_{max}/cm^{-1} 3319 (br w), 2920 (br w), 1719 (s), 1537 (m).

LRMS: (ESI) m/z 542 ([^{81}M+H]$^+$), 540 ([^{79}M+H]$^+$), 366 ([$C_{12}H_{18}{}^{81}BrN_3O_5$+H]$^+$), 364 ([$C_{12}H_{18}{}^{79}BrN_3O_5$+H]$^+$), 323 ([$C_{10}H_{13}{}^{81}BrN_2O_5$+H]$^+$), 321 ([$C_{10}H_{13}{}^{79}BrN_2O_5$+H]$^+$).

HRMS: (ES+) calcd for [$C_{23}H_{30}{}^{79}BrN_3O_7$+H]$^+$ [^{79}M+H]$^+$ 540.13399 (5 d.p.), observed 540.1336 (4 d.p.)

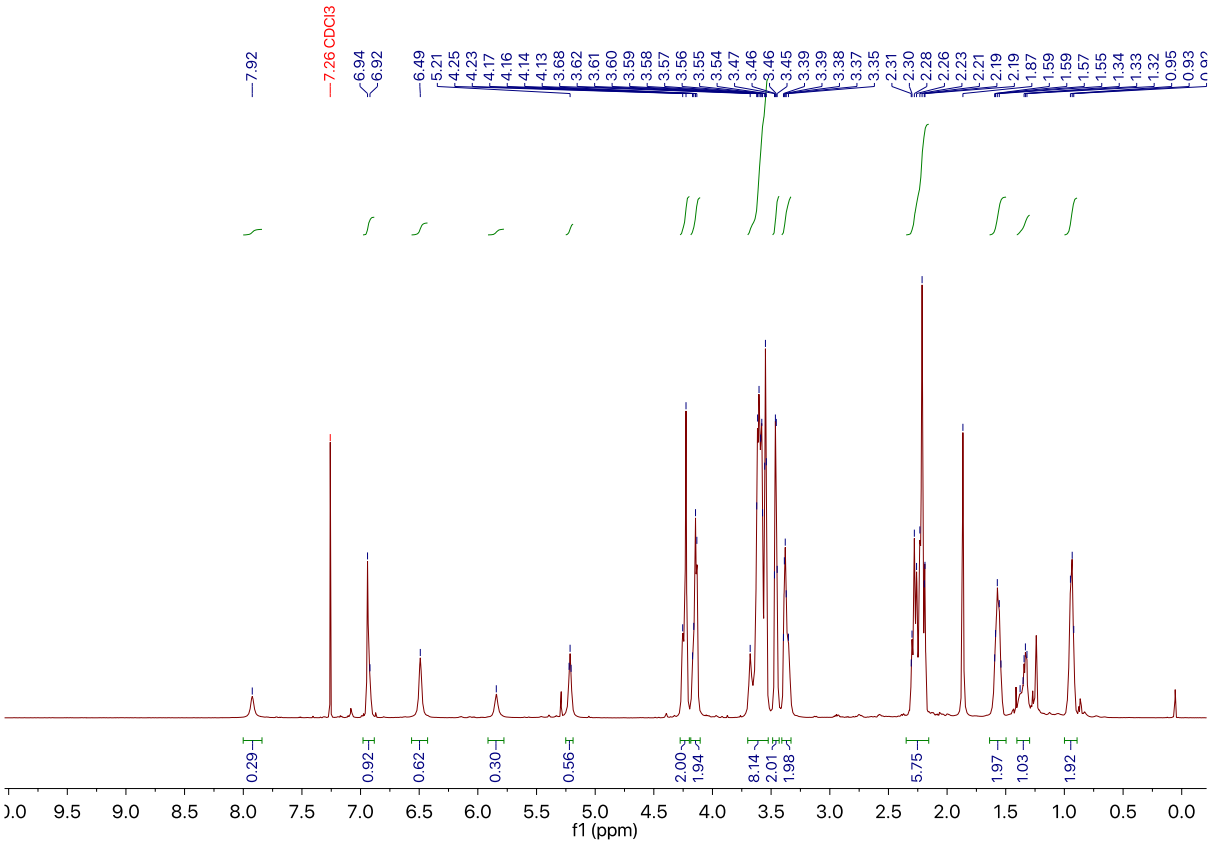

Figure S4. Zoomed in ^{1}H spectra of MBM-BCN.

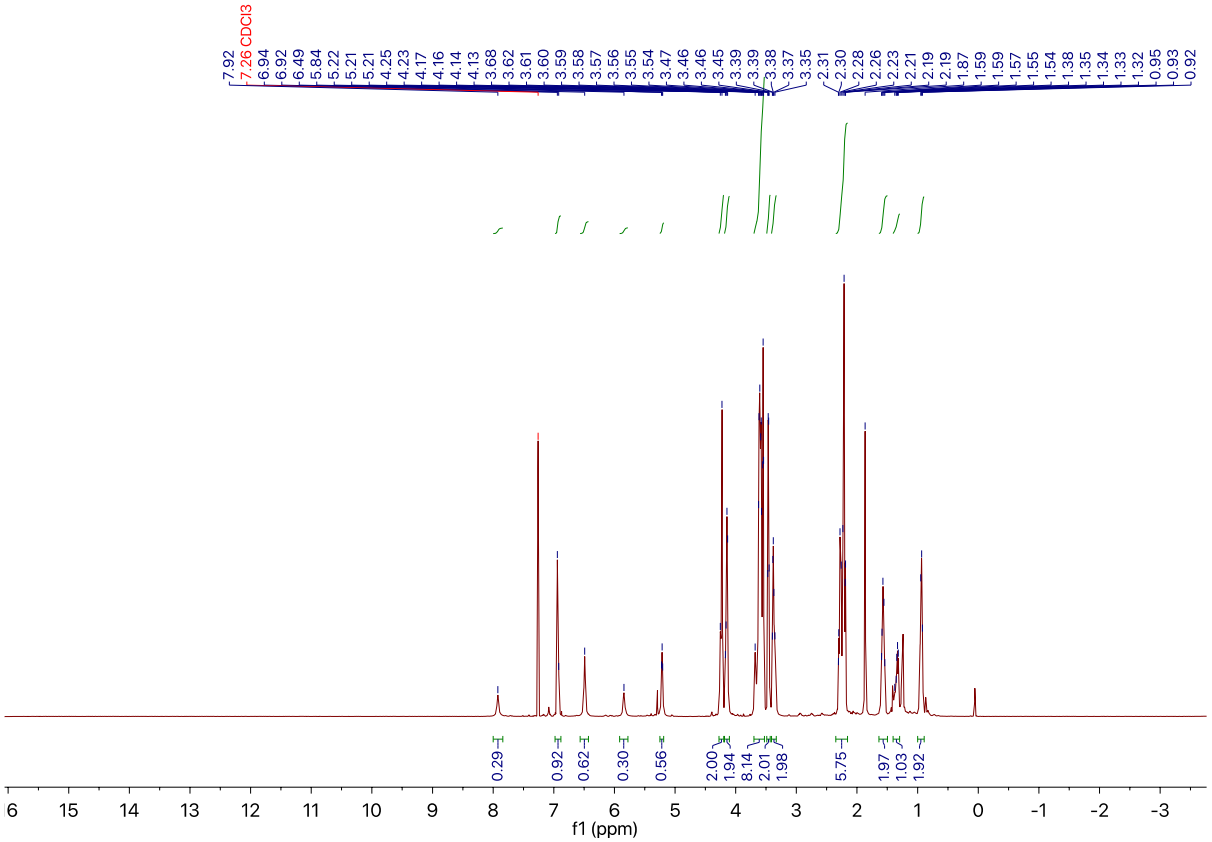

Figure S5. Zoomed out ^{1}H spectra of MBM-BCN.

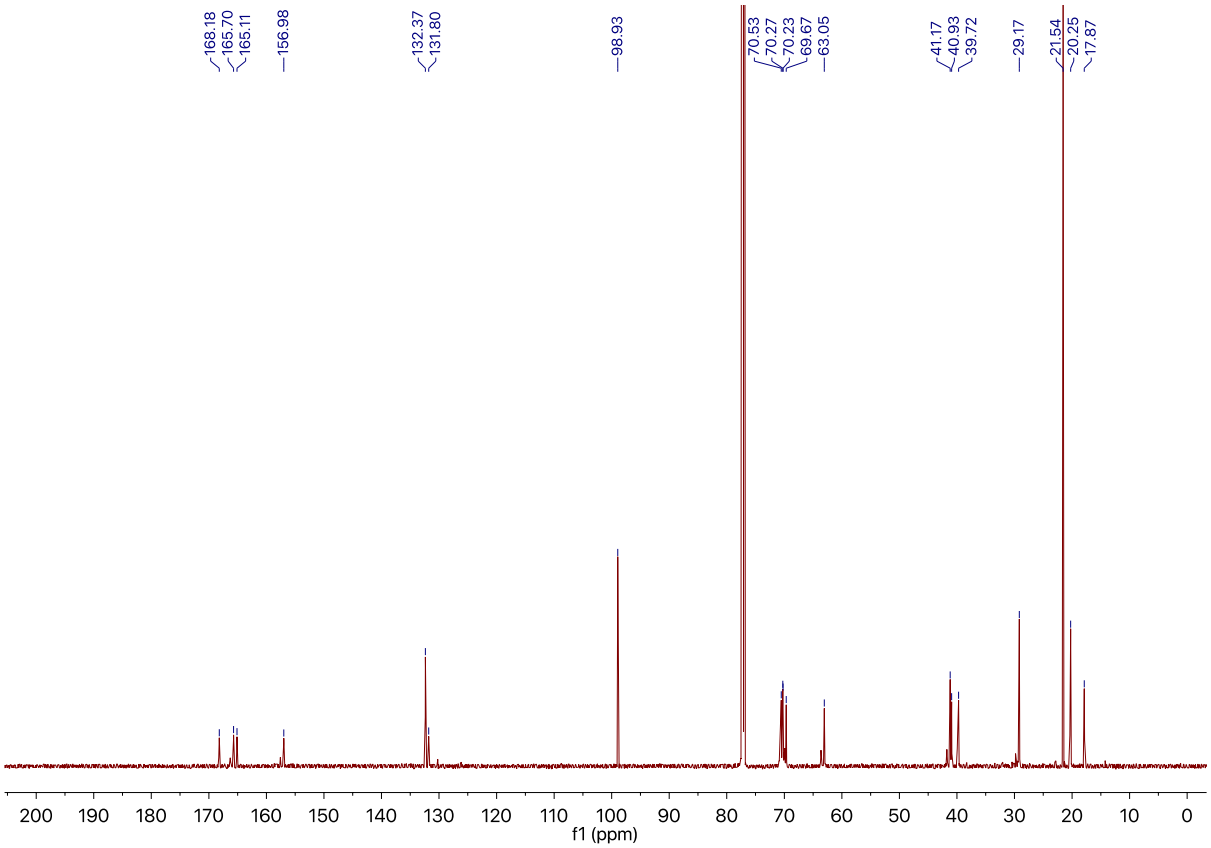

Figure S6. Zoomed in ^{13}C spectra of MBM-BCN.

10.3. Synthesis of MMAE-azide

2-(2-(2-(2-((1,3-Dioxoisoindolin-2-yl)oxy)ethoxy)ethoxy)ethoxy)ethyl (4-nitrophenyl) carbonate (3)

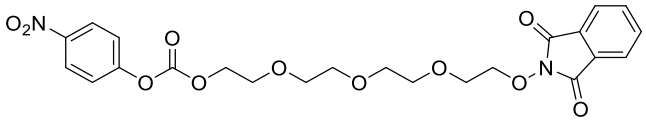

Prepared according to a literature synthesis [48].

MMAE phthalimide (4)

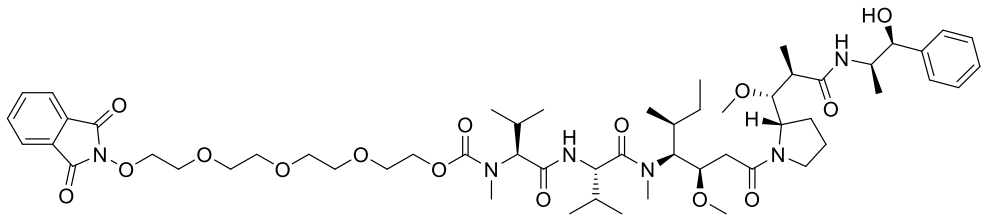

To a dry vial with a stirring solution of compound **3** (0.011 g, 0.021 mmol, 1.5 eq.) in anhydrous DMF (1 mL) was added MMAE (10 mg, 0.014 mmol, 1.0 eq.) and 1-hydroxybenzotriazole (1 mg, 0.0069 mmol, 0.50 eq.) after 5 min dry pyridine (2 mg, 0.028 mmol, 2.0 eq.) was added. After 8 h the solvent was removed *in vacuo*. Purification of the crude product by flash column chromatography (DCM : 0.5% - 4% MeOH)

provided the title compound as a slightly white oil (14 mg, 0.013 mmol, 94%). HRMS (ESI) m/z [M + K]+ calcd for $C_{56}H_{86}KN_6O_{15}$+: 1121.5783 Found: 1121.5788.

MMAE alkoxyamine (5)

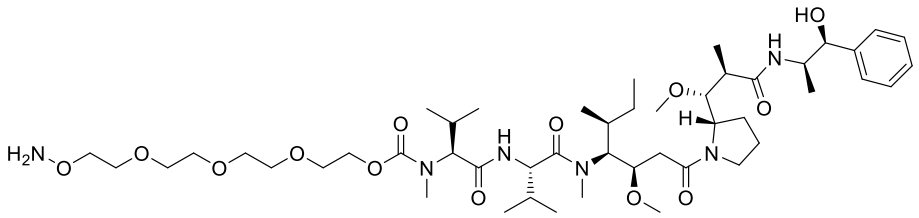

To a dry vial with a stirring solution of compound **4** (14.1 mg, 0.013 mmol, 1.0 eq.) in ethanol (1 mL) was added hydrazine (5.8 mg, 0.182 mmol, 14 eq.). The solution was stirred at RT overnight. The solvent was removed *in vacuo*. Purification of the crude product by flash column chromatography (DCM : 0.5% - 5% MeOH) provided the title compound as a slightly white oil (11.7 mg, 0.012 mmol, 94%). HRMS (ESI) m/z [M + K]+ calcd for $C_{48}H_{84}KN_6O_{13}$+: 991.5728 Found: 991.5725.

MMAE-azide (6)

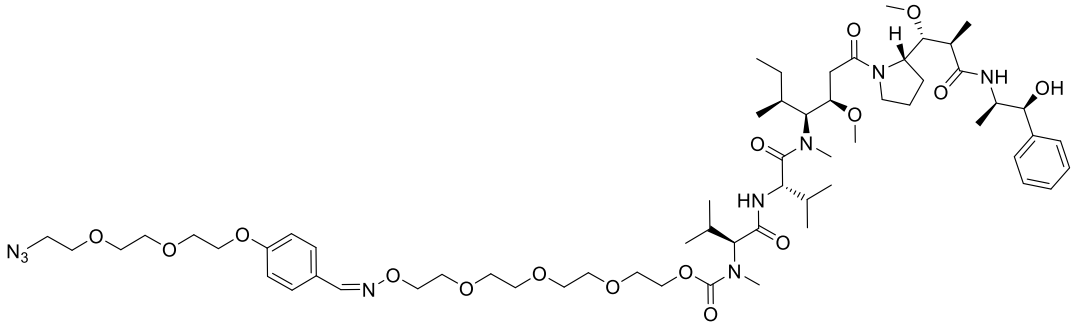

To a dry vial with a stirring solution of compound **5** (7.0 mg, 0.007 mmol, 1.0 eq.) in dry MeOH was added triethylamine (0.0029 g, 0.022 mmol, 3.0 eq.) and 4-(2-(2-(2-azidoethoxy)ethoxy)ethoxy)benzaldehyde (0.0033 g, 0.0012 mmol, 1.6 eq.). The solution was stirred at RT overnight and the solvent was removed *in vacuo*. Purification of the crude product by flash column chromatography (DCM : 0.5% - 5% MeOH) provided the title compound as a slightly white oil (8.1 mg, 0.0067 mmol, 91%). HRMS (ESI) m/z [M + K]+ calcd for $C_{61}H_{100}N_9O_{16}$+: 1214.7283 Found: 1214.7285. Purity was confirmed by RP C18 HPLC (Figure S7).

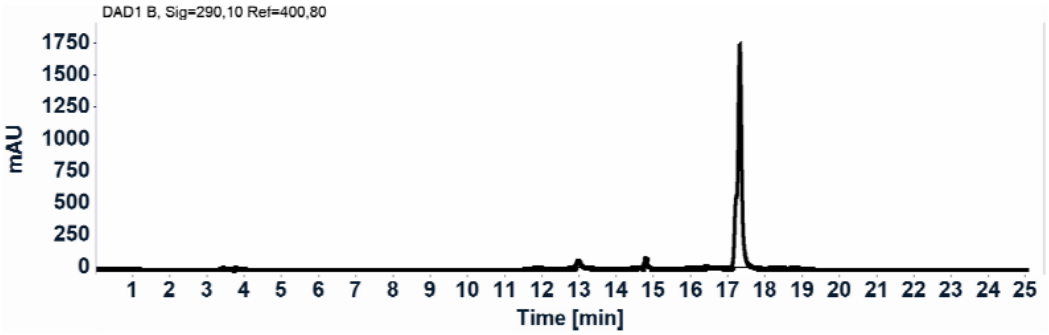

Figure S7. HPLC RP C18 chromatogram showing purity of MMAE-azide.

The acid cleavability of MMAE-azide was investigated by incubating overnight at different pHs in a citric acid phosphate buffer (100 mM) with 100 mM NaCl at 37°C. Samples were then analyzed on analytical C18 HPLC and chromatograms were integrated to find amount left of MMAE-azide.

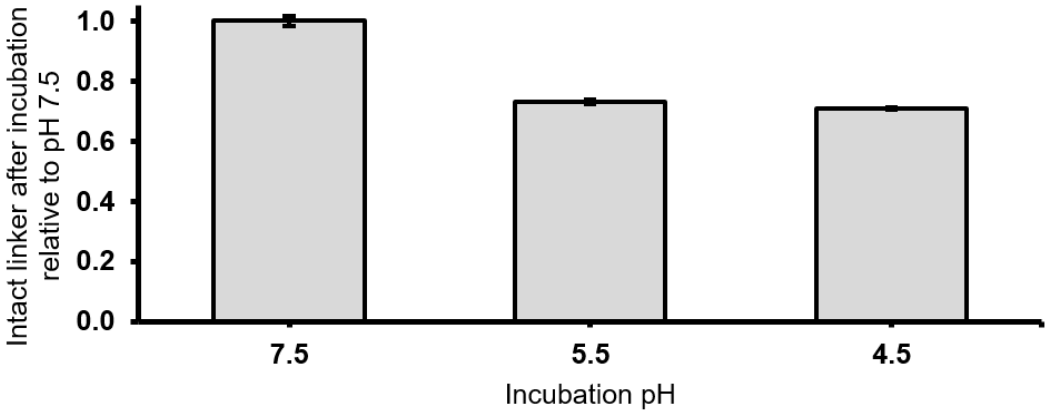

Figure S8. pH-dependent cleavage of MMAE-azide. N=3 independent experiments, error bars indicate SEM.